A MONTE CARLO INVESTIGATION OF THE PLANAR
LEBWOHL–LASHER LATTICE MODEL

C. CHICCOLI and P. PASINI

I.N.F.N. Sez. di Bologna and C.N.A.F., Via Mazzini 2, 40138 Bologna, Italy

C. ZANNONI

*Dipartimento di Chimica Fisica ed Inorganica, Universitá, Viale Risorgimento 4,
40136 Bologna, Italy*

A Monte Carlo computer simulation of a planar version of the Lebwohl–Lasher model is presented. The model consists of a set of interaction centres forming a simple square lattice. The pair potential is nearest-neighbours, attractive, and varies as a second Legendre polynomial of the relative orientation between the two particles. Five lattice sizes, 5×5, 10×10, 20×20, 60×60 and 80×80, of this two-dimensional system have been simulated with Monte Carlo and periodic boundary conditions. A study of the orientational pair correlation function indicates a power law decay in the ordered phase and an exponential decay above the pseudo-transition temperature. Our results are consistent with the absence of a true phase transition but also indicate a low-temperature phase with long short-range order. Comparisons are made with one existing simulation and with the mean field theory results.

1. Introduction

The Lebwohl–Lasher model[1] has become the prototype for a number of studies of the orientational phase transition in nematic liquid crystals. In the original version of the model, particles are placed at the sites of a cubic lattice and they are allowed to interact through the attractive nearest-neighbours pair potential

$$U_{ij} = - \varepsilon_{ij} P_2(\cos \beta_{ij}) , \tag{1}$$

where β_{ij} measures the angle between the symmetry axes of the two molecules and ε_{ij} designates the strength of the interaction. Various Monte Carlo simulations[2-11] including a rather large one on a $30 \times 30 \times 30$ lattice[11] indicate that the Lebwohl–Lasher model possesses a phase transition at a

dimensionless temperature $T^* = kT/\varepsilon \simeq 1.1232$ [11]). The phase transition appears to be a very weak first order transition. On a more general level the possibility of having a true orientational transition is certainly not forbidden in the standard Lebwohl–Lasher model with dimensionality $d = 3$ for the lattice and $n = 3$ for the orientational space. In the terminology used for magnetic systems the latter dimension would be called a spin dimensionality[12-16]). As it is often the case with successful models the original system has proliferated and has given rise to a whole family. Thus models with molecules reorienting in a plane ($n = 2$ analogous) have been investigated for linear, $d = 1$ [17]), planar, $d = 2$ [18]) and cubic, $d = 3$ lattices[19]). As for molecules reorienting in three-dimensional space, a linear ($d = 1$, $n = 3$) and a planar ($d = 2$, $n = 3$) lattice have been discussed by Vuillermot and Romerio[20,21]). They were able to provide an analytical solution showing, as expected, the absence of a true transition for the linear lattice[20]).

Here we wish to study with the aid of Monte Carlo simulations a two-dimensional lattice of particles interacting through eq. (1). We shall call this the planar Lebwohl–Lasher model. This system cannot have conventional long-range order according to a rigorous study based on a generalized version of Mermin–Bogolyubov inequality proved by Vuillermot and Romerio[21]) for a class of models with Gegenbauer polynomial[22]) interactions. This category of models contains the classical Heisenberg models and the present Lebwohl–Lasher model. However, after the now classical Kosterlitz–Thouless finding of topological phase transitions in a large class of O(2), $n = 2$ models where traditional phase transition is forbidden it seems interesting to collect some computer experimental evidence on other systems. While for particles moving on a plane the presence of vortices seems now fairly well established, the problem of existence of phase transition in planar systems with O(3) interactions is not completely settled[23]). A system particularly studied has been the Heisenberg model where the O(3) interactions are of rank one. There the possibility of topological defects similar to Kosterlitz–Thouless ones (instantons) has been investigated. However, while there have been many computer simulation studies of the Heisenberg lattice[25,26]) we are aware of only one study reported for the planar second rank model equation (1) [5]). This was a Monte Carlo simulation of a relatively small 20×20 system performed by Mountain and Ruijgrok as part of an interesting Monte Carlo study of various planar Lebwohl–Lasher lattices[5]). In this study Mountain and Ruijgrok exclude a first order phase transition and suggest that ordering takes place through a higher order mechanism. Here we wish to collect some MC data on the O(3), $d = 2$, second rank model for various systems of different sizes. In particular we wish to provide some evidence on the existence and character of a pseudo-orientational phase transition and on the type of order decay with

distance. The possibility of observing ordered liquid crystal systems in two dimensions, e.g. on surfaces, would be linked to a decay slow enough to allow formation of patches susceptible of experimental observation. For this purpose studying various systems of increasing size is essential and has been one of the aims here.

2. The simulations

We have studied five systems of different sizes. A standard Metropolis Monte Carlo method with periodic boundary conditions[2,13–16]) has been employed to generate equilibrium configurations. The simulation at the lowest temperature studied for each of the five cases was started from a completely aligned system. The simulations at the other temperatures have been normally run in cascade starting from an equilibrium configuration at a nearby lower temperature. An additional simulation has been run for the 20×20 lattice starting from a random (isotropic) configuration and cooling down. This has been done with the purpose of looking for hysteresis effects as we shall discuss later on. The orientation of each particle is stored as $\cos \beta$ and α, where β and α are the polar angles of the symmetry axis of each particle. The configuration of the system is thus given by the set of N such orientations $\{\alpha_i, \beta_i\}$ where N is the number of particles. We update one particle at a time and as usual we shall call a cycle a set of N attempted moves. A new configuration is generated by randomly choosing a particle amongst those that we have not yet attempted to move during the current lattice sweep with a shuffling algorithm[11]). The orientation of the chosen particle is then changed by generating new uniformly distributed random values of the variables $\cos \beta$ and α. A satisfactory rejection ratio is achieved for our temperature range even with these potentially large orientational jumps. In every simulation a minimum of 5 000 cycles has been used for equilibrium and thus rejected when calculating averages. Runs were typically between 12 000 and 20 000 cycles. Longer runs, from 60 000 to 90 000 cycles, have been run for the four temperatures near the heat capacity anomaly of the 80×80 lattice. Any property of interest, A, is evaluated at every cycle. After a certain number of cycles m_J (typically between 1 000 and 2 000) an average A^J is calculated thus effectively coarse-graining the trajectory. A further grand average is then computed as the weighted average over M such supposedly uncorrelated segments. The attendant weighted standard deviation from the average σ_A is also calculated and gives the error estimates reported here for observables.

We have calculated for each simulation energy, second and fourth rank order parameters. Pair correlation coefficients again of second and fourth rank have been calculated at selected temperatures for the 20×20 and 80×80 lattices. The heat capacity of the system has been evaluated by differentiation of the internal energy.

3. Results and discussion

3.1. *Energy*

The energy of the system is calculated as a sum of pair interactions as in eq. (1). Thus

$$\langle U_N \rangle = -\tfrac{1}{2} \sum_{i=1}^{N} \sum_{j=1}^{N} \varepsilon_{ij} \langle P_2(\cos \beta_{ij}) \rangle ; \quad \text{with } i \neq j$$

$$= -\frac{N}{2} z\sigma_2 , \tag{2}$$

where $z = 4$ is the coordination number and $\sigma_2 = \langle P_2(\cos \beta_{12}) \rangle$ is a short-range order parameter averaged over neighbour particles. The average dimensionless single particle energies $U^* = \langle U \rangle / N\varepsilon$ at the set of reduced temperatures $T^* = kT/\varepsilon$ studied are reported in fig. 1. They are quite similar even for our smallest and largest systems, thus it seems that short-range order effects are settled very quickly. Examining fig. 1 we see that the curves are essentially
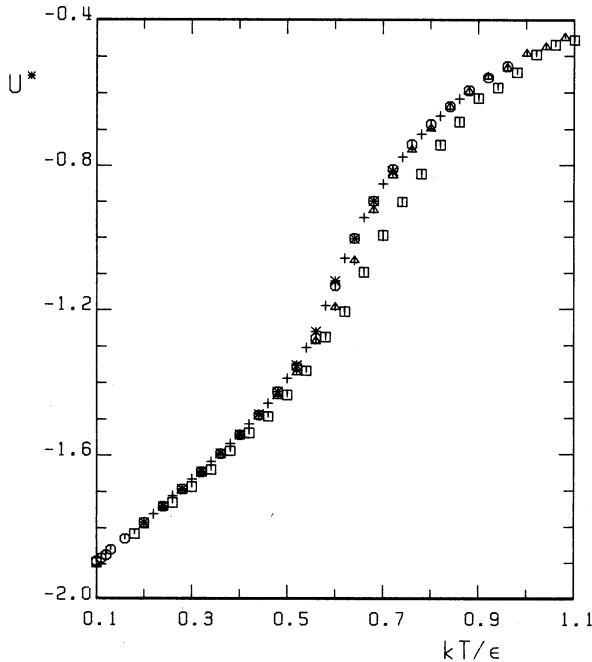

Fig. 1. The single particle energy $U^* = \langle U \rangle / N\varepsilon$ versus dimensionless temperature $kT/\varepsilon = T^*$ for the square Lebwohl–Lasher lattice of size 5×5 (squares), 10×10 (triangles), 20×20 (circles), 60×60 (plus), 80×80 (stars).

superimposable from the lowest temperatures up to $T^* \simeq 0.6$ and that they deviate a little more at high temperatures for the various systems examined.

3.2. *Heat capacity*

The dimensionless heat capacity C_V^* is obtained here by differentiating the average energy with respect to temperature as previously described[27]). In brief, the energy values are interpolated and smoothed using a five-point orthogonal formula before performing the numerical differentiation[27,28]) with an inversion method[29]). The results are presented in fig. 2 for the various sizes studied. We see that heat capacity is insensitive to increasing the system size from 100 to 6 400 particles. This contrasts profoundly with the behaviour found in the three-dimensional Lebwohl–Lasher model[11]). There a marked systematic sharpening of the heat capacity peak with increasing lattice size is observed as it is expected for a true phase transition. The pseudo-transition
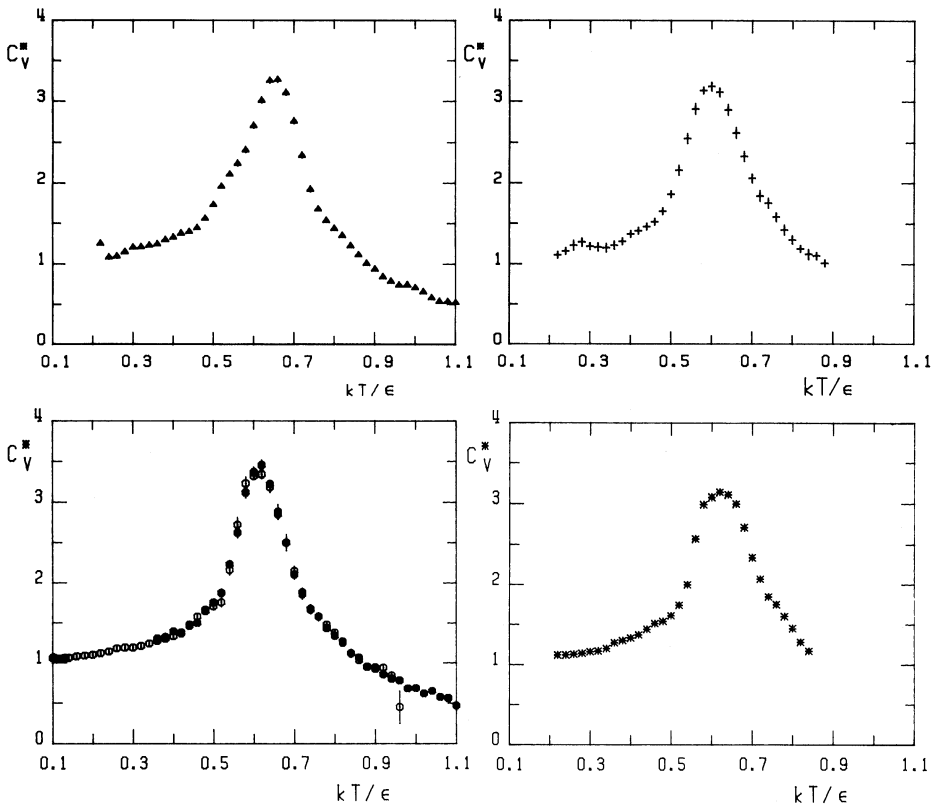

Fig. 2. The heat capacity C_V^* obtained from differentiation of energy plotted versus dimensionless temperature kT/ε. Symbols for the various lattice sizes are as in fig. 1.

The pseudo-transition temperatures T_C^* and T_D^* obtained from the heat capacity and order parameter derivatives. The peak values C_{max}^* and $[d\langle P_2 \rangle / dT^*]_{min}$ are reported. The results correspond to the five lattice sizes ($L \times L$) considered.

L	C_{max}^*	T_C^*	$[d\langle P_2 \rangle / dT^*]_{min}$	T_D^*
5	2.7 ± 0.2	0.68 ± 0.01	-1.5 ± 0.3	0.68 ± 0.01
10	3.3 ± 0.1	0.66 ± 0.01	-2.8 ± 0.2	0.66 ± 0.01
20	3.3 ± 0.1	0.62 ± 0.01	-4.1 ± 0.3	0.62 ± 0.01
20[a]	3.5 ± 0.1	0.62 ± 0.01	-4.2 ± 0.3	0.62 ± 0.01
60	3.2 ± 0.1	0.60 ± 0.01	-5.0 ± 0.2	0.56 ± 0.01
80	3.14 ± 0.01	0.62 ± 0.01	-5.1 ± 0.1	0.58 ± 0.01

[a] Simulation run in a cooling sequence.

temperature, i.e. the temperature at which the maximum of the heat capacity occurs decreases as the size increases as we can see from table I.

According to finite scaling[30] the transition temperature $T_C(L)$ for a system with linear dimension L is linked to the true one by the scaling relation[15]

$$T_C(L) \approx T_C(\infty) + aL^{-1/\nu} , \quad L \gg 1 , \tag{3}$$

where a is a constant for the system and boundary conditions chosen and ν is the correlation length exponent. In practice a trial $\nu = 1$ is often assumed in view of the uncertainty in the experiment and of the fact that ν is of course unknown[15]. In fig. 3 we show a finite size scaling plot of T_C^*. The heat capacity
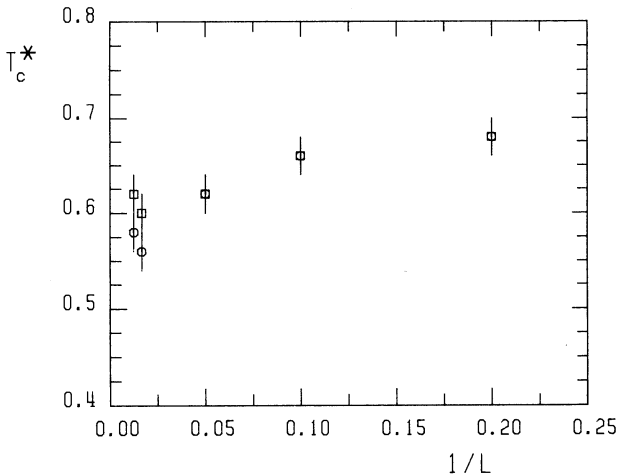

Fig. 3. A plot of the temperature of the heat capacity anomaly maximum T_C^* plotted vs. inverse of the lattice linear size L (squares). The circles correspond to the same scaling plot for the order parameter derivative peak.

results (square symbols in fig. 3) indicate a low-temperature shift with size, even if this effect becomes at best very modest for the two larger systems. We conclude that on the basis of C_V^* alone we can just confirm the theoretical expectations about the absence of a true phase transition.

3.3. Order parameters

In any problem involving liquid crystals the calculation of order parameters is of central importance. Here the order parameters represent expansion coefficients of the expansion of the singlet distribution $P(\cos \beta)$ with β the angle of the particle axis and the preferred orientation (director) in a Legendre polynomials[22]) basis. We have determined the first two nontrivial order parameters as follows.

The second rank order parameter $\langle P_2 \rangle_\lambda$ is calculated as usual in the computer simulation of systems with periodic boundary conditions[8,31]) from the average over cycles of the largest eigenvalue, λ_3, of the ordering matrix $\mathbf{Q}$,
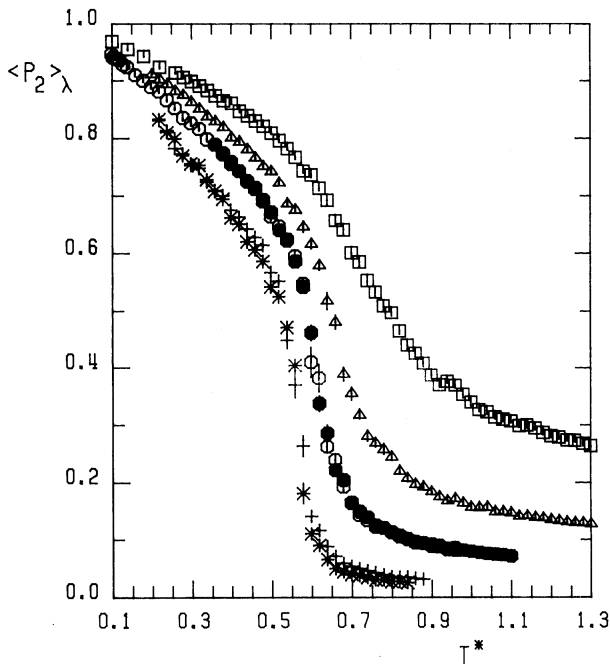

Fig. 4. The second rank order parameter $\langle P_2 \rangle_\lambda$ for the six systems studied plotted vs. dimensionless temperature T^*. Here $\langle P_2 \rangle_\lambda$ is obtained from the largest eigenvalue of the ordering matrix as recalled in the text. Simulations from a heating sequence for 5×5 (squares), 10×10 (triangles), 20×20 (empty circles), 60×60 (plus), 80×80 (stars) are shown. An additional 20×20 simulation run in a cooling sequence is also shown (full circles).

$$Q_{ab} = \langle q_{i,a}q_{i,b} - \tfrac{1}{3}\,\delta_{a,b}\rangle_S\,, \tag{4}$$

where, e.g., $q_{i,x}$ stand for the x component of the unit vector q_i specifying the orientation of the ith particle. The matrix is computed and diagonalized at every cycle and the average $\langle\cdots\rangle_S$ extends to all the particles in the system. A discussion of this and other definitions of $\langle P_2\rangle$ was given in ref. 11. The order parameter $\langle P_2\rangle_\lambda$ obtained in this way is plotted in fig. 4 against temperature for all the systems we have studied.

We notice first that for small lattices the curves change quite noticeably with size. For instance the 5×5 and 10×10 systems have an order parameter quite high and different from one another in the isotropic phase. However, the differences become less apparent as the size increases. This behaviour is not too surprising[32]) since it is partly dictated by the low-temperature limit of one and the high-temperature limit of $\mathcal{O}(1/N)$ [33]) for $\langle P_2\rangle_\lambda$. Very little differences are observed between a 60×60 and an 80×80 magnitude. We notice also the absence of hysteresis in the 20×20 system. Indeed the $\langle P_2\rangle_\lambda$ for the set of heating (empty circles) or cooling (full circles) experiments are in excellent agreement through the whole temperature range. The slope of the order parameter vs. temperature curve depicts the potential occurrence of a transition or a rapid change of the order parameter. The temperature derivative of the order parameter can be viewed as a rough long-range indicator of the transition[27]) to be compared with the short-range indicator, i.e. the heat capacity. We have thus computed these derivatives following the same smoothing–interpolation procedure as previously introduced. The values of the long-range pseudo-transition temperatures obtained are reported in table I. We see that there is excellent agreement between the long-range and the short-range indicators for sizes up to 20×20. For larger sizes the transition temperature as signalled by the order parameter derivative is slightly lower than that obtained from C_V^*. In the analysis of simulations data for the three-dimensional Lebwohl–Lasher model[11]) it was found quite useful to examine histograms of the occurrences of $\langle P_2\rangle_\lambda$ during the simulation. The rationale is that the shape of the distribution of order parameters can yield indications of the occurrence of a phase transition in terms of changes of asymmetry. Moreover an estimate of the extent of fluctuations in $\langle P_2\rangle_\lambda$ can be obtained from the width of distribution. In fig. 5 we present histograms of the $\langle P_2\rangle_\lambda$ distribution for four temperatures across the heat capacity anomaly of the 80×80 system. We see that even for this fairly large system the change from order to disorder is quite smooth. Fluctuations become very large at $T^* = 0.58$ and the spread of $\langle P_2\rangle_\lambda$ values really shows that this is more informative than just looking at the average value.

The calculation of the fourth rank order parameter $\langle P_4\rangle_\lambda$ was performed
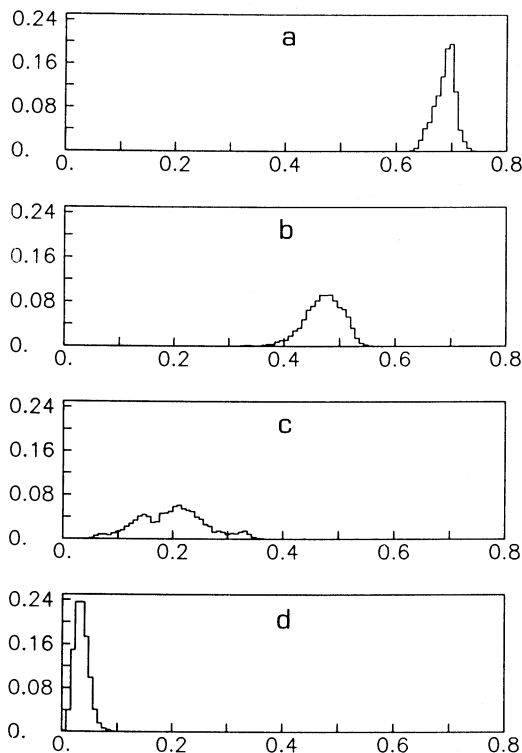
Fig. 5. Histograms of frequency of occurrence of the second rank order parameter $\langle P_2 \rangle_\lambda$ during simulations on the 80×80 lattice at $T^* = 0.40$ (a), 0.54 (b), 0.58 (c), 0.72 (d).

according to the algorithm we have previously proposed[11,27]). The values for the fourth rank order parameter obtained for our simulation are reported as a function of temperature in fig. 6. The fourth rank order parameter shows again a convergence with sizes above 60×60.

3.4. *Orientational pair correlations*

The two-particle angular correlations coefficients $G_L(r)$ describe a set of expansion coefficients of the rotationally invariant pair correlation function[2,11]). The calculation is quite time-consuming and represents a relevant percentage of the total time spent in the simulation (roughly a fourth). We have calculated the first two angular pair correlation coefficients G_2 and G_4 for all the temperatures of the 20×20 system studied in the heating sequence. For the 80×80 system the pair correlations have been computed for a few selected temperatures only. In fig. 7 we show as an example $G_2(r)$ of the large lattice for two temperatures, respectively below and above the heat capacity anomaly. When using periodic boundary conditions, every distance-dependent property
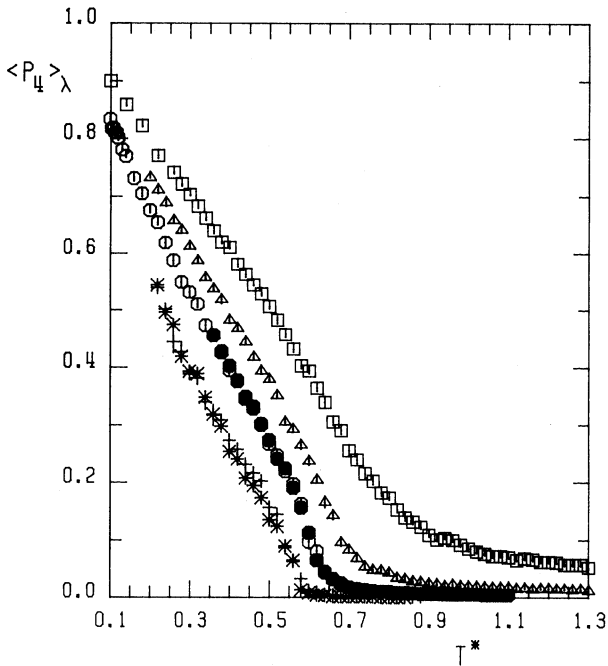
Fig. 6. The fourth rank order parameter $\langle P_4 \rangle_\lambda$ obtained as described in the text plotted vs. temperature T^* shown for the various systems studied (symbols as in fig. 4).
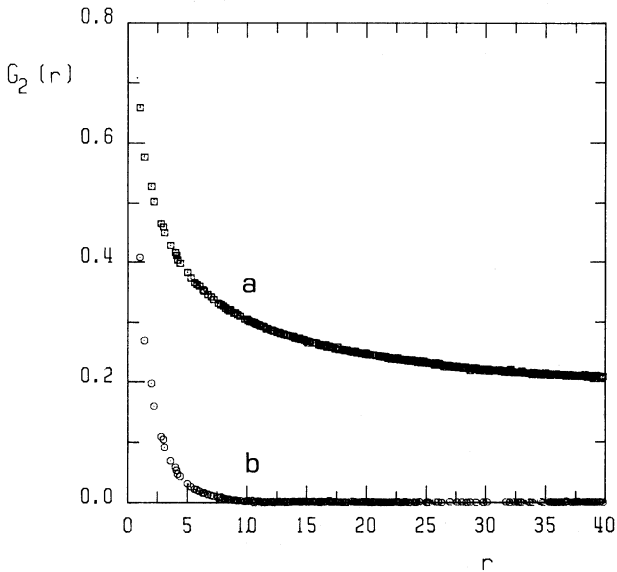
Fig. 7. The second rank pair correlation coefficient $G_2(r)$. The example case shown is for the 80×80 lattice at temperatures $T^* = 0.54$ (a) and $T^* = 0.72$ (b).

is determined modulo the box length so the correlations will grow eventually with separation. Here we show the curves for distances starting from the nearest-neighbour one and up to half of the box length. The pair coefficients $G_L(r)$ start from one and in a uniformly aligned system with true long-range order would tail off to essentially $\langle P_L \rangle^{2\ 2})$. This is what happens in the three-dimensional Lebwohl–Lasher model[11]) below the nematic–isotropic transition. On the other hand, a system like the one-dimensional Lebwohl–Lasher model where a phase transition does not exist should have theoretically an exponentially decaying correlation[20,21]). We show elsewhere that this is indeed the case[32]). We see that below T_C^* a slow decay is observed while the decay is very fast above T_C^*. Obviously it is difficult to assess an appropriate functional form at eyesight. We have thus performed a nonlinear least-square fitting of all the second rank correlation coefficients available to the following two expressions:

  (a) exponential decay to a plateau,

$$G_2(r) = (1 - A_e) e^{-k_e r} + A_e ; \tag{5}$$

  (b) power law decay to zero,

$$G_2(r) = A_p / r^{k_p} . \tag{6}$$

In practice we perform the nonlinear least-square fit to raw data up to a certain cut-off length L_f. We have found that the exponential law gives a better fit for the results above T_C^*, while the power law gives a better representation of the data below T_C^*. In fig. 8 we present a plot of our data for the power law decay constant k_p for the 20×20 system at temperatures below T_C^*. We see that the decay length (inverse of k_p) increases regularly as the temperature decreases, tending to infinity ($k_p = 0$) at $T^* = 0$. The points obtained for the 80×80 lattice shown for three cut-offs ($L_f = 10, 20, 40$) confirm this behaviour. Results for the different cut-offs are in very good agreement except near the order–disorder anomaly where the power-law fit is poor anyway. We also notice that the results from the 20×20 simulation are in agreement with those for the larger system, especially at low temperatures. It is tempting to compare our results for k_p with the values predicted by the Kosterlitz–Thouless theory. In particular Kosterlitz–Thouless predict that $k_p = 1/4$ at the vortex unbinding transition. If we look at the data in fig. 8 and only consider points up to temperatures where a consistent fit, with good agreement between different cut-offs, is obtained (i.e. say up to $T^* \approx 0.55$) then a value of k_p not too different from the Kosterlitz–Thouless one is obtained. It should be noticed, however, that in this O(3) model the standard vortices do not represent a true
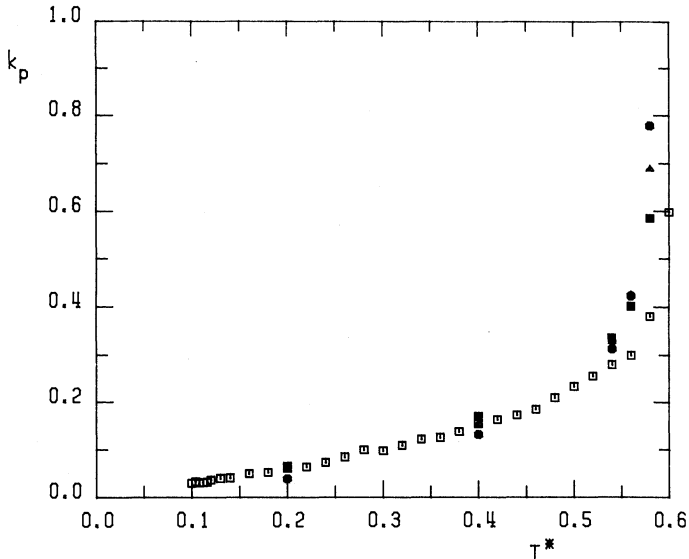
Fig. 8. The decay constant k_p in a power law fitting of $G_2(r)$ vs. r. Data are shown for the 20×20 planar lattice (squares) with a cut-off distance at $r = 9$ and for the 80×80 lattice with a cut-off at $r = 10$ (full squares), $r = 20$ (triangles), $r = 40$ (full circles). Results are plotted at the available dimensionless temperatures T^*.

topological defect, since the molecular orientation vector can point outside the plane. After the findings of Belavin and Polyakov[23b] the presence and the role of instantons has been investigated in the O(3) Heisenberg model[24,26] but it is probably fair to say that their importance in lattice model is still being discussed[26b]. We have also investigated the presence of ordered structures but we were unable to observe well-characterized structures.

4. Conclusions

Where comparison is possible our results are in agreement with those of Mountain and Ruijgrok[5], while extending them to larger size systems. In addition the finer temperature grid allows us to improve the determination of the heat capacity anomaly temperature. Investigation of the size dependence of the results shows that some of them, and particularly the order parameter, change when going from the 20×20 to the 60×60 and 80×80 lattices. We think the calculation and analysis of pair correlation functions is particularly useful in trying to assess the extent and type of ordering present in the system. Performing this kind of investigation we find that the system does not exhibit a true phase transition, in accordance with theoretical results. However, the system presents long short-range order with a decay of the pair correlation

function which is exponential above a characteristic temperature T_C^* and a much slower power law decay below. Determining the nature of ordering in this temperature region would require further investigations, a bit like in the Heisenberg model case[24-26]). After all, even though the rigorous arguments tell us what cannot happen in an infinitely large lattice, they do not say very much about alternative allowed kinds of ordering in finite although possibly large systems.

Acknowledgments

References

1) P.A. Lebwohl and G. Lasher, Phys. Rev. A **6** (1972) 426.
2) C. Zannoni, in: The Molecular Physics of Liquid Crystals, G.R. Luckhurst and G.W. Gray, eds. (Academic, New York, 1979), chap. 9.
3) H.J.F. Jansen, G. Vertogen and J.G.J. Ypma, Mol. Cryst. Liquid Cryst. **38** (1977) 87.
4) H. Meirovitch, Chem. Phys. **21** (1976) 251.
5) R. Mountain and Th. W. Ruijgrok, Physica **89A** (1977) 522.
6) C. Zannoni and M. Guerra, Mol. Phys. **44** (1981) 849.
7) R.L. Humphries and G.R. Luckhurst, Proc. Roy. Soc. A **382** (1982) 307.
8) G.R. Luckhurst and P. Simpson, Mol. Phys. **47** (1982) 251.
9) G.R. Luckhurst, S. Romano and P. Simpson, Chem. Phys. **73** (1982) 337.
10) C. Zannoni, J. Chem. Phys. **84** (1985) 424.
11) U. Fabbri and C. Zannoni, Mol. Phys. **58** (1986) 763.
12) H.E. Stanley, Introduction to Phase Transitions and Critical Phenomena (Oxford Univ. Press, London, 1971).
13) K. Binder, Monte Carlo Methods in Statistical Physics, K. Binder, ed. (Springer, Berlin, 1979), chap. 1 and refs. therein.
14) D.P. Landau, Applications of the Monte Carlo Method in Statistical Physics, K. Binder, ed. (Springer, Berlin, 1984), chap. 3 and refs. therein.
15) O.G. Mouritsen, Computer Studies of Phase Transitions and Critical Phenomena (Springer, Berlin, 1984).
16) K. Binder, J. Comput. Phys. **59** (1985) 1.
17) J.Y. Denham, R.L. Humphries and G.R. Luckhurst, Mol. Cryst. Liquid Cryst. Lett. **41** (1977) 67.
18) J.Y. Denham, G.R. Luckhurst, C. Zannoni and J.W. Lewis, Mol. Cryst. Liquid Cryst. Lett. **60** (1980) 185.
19) H. Zewdie, Ph. D. thesis, University of Southampton (1986).
20) P.A. Vuillermot and M.V. Romerio, J. Phys. C **6** (1973) 2922.

21) P.A. Vuillermot and M.V. Romerio, Commun. Math. Phys. **41** (1975) 281.
22) M. Abramowitz and I.A. Stegun, eds., Handbook of Mathematical Functions (Dover, New York, 1964).
23a) See e.g. A.Z. Patasinskij and V.L. Pokrovskij, Teoria delle Fluttuazioni nelle Transizioni di Fase (Editori Riuniti, Roma, 1985).
23b) A.A. Belavin and Polyakov, JETP Lett. **22** (1975) 245.
24) J. Tobochnik and G.V. Chester, Phys. Rev. B **20** (1979) 3761.
25) S. Miyashita, H. Nishimori, A. Kuroda and M. Suzuki, Progr. Theor. Phys. **60** (1978) 1669.
26a) S.H. Shenker and J. Tobochnik, Phys. Rev. B **22** (1980) 4462.
26b) F. Fucito and S. Solomon, Phys. Lett. B **134** (1984) 230.
27) C. Chiccoli, P. Pasini and C. Zannoni, Liquid Cryst. **2** (1987) 39.
28) H.C. Hershey, J.L. Zakin and R. Simha, Industr. Eng. Chem. Fundam. **6** (1967) 413.
29a) A. Tikhonov and V. Arsenine, Methodes de Resolution de Problemes Mal Poses (MIR, Moscow, 1976).
29b) B. Rust, W.R. Burrus and C. Schneeberger, Comms. ACM **9** (1966) 381.
30) M.E. Fisher and A.E. Ferdinand, Phys. Rev. Lett. **29** (1967) 169.
31) J. Viellard-Barron, Mol. Phys. **28** (1974) 809.
32) C. Chiccoli, P. Pasini and C. Zannoni, Liquid Crystals, in press.
33) R. Eppenga and D. Frenkel, Mol. Phys. **52** (1984) 1303.